Journal of Breast Cancer

J Breast Cancer 2016 September; 19(3): 231-241 http://dx.doi.org/10.4048/jbc.2016.19.3.231

ORIGINAL ARTICLE

Cell-in-Cell Death Is Not Restricted by Caspase-3 Deficiency in MCF-7 Cells

Shan Wang[1,2,3], Meifang He[4], Linmei Li[1,2,3], Zhihua Liang[1,2,3], Zehong Zou[1,2,3], Ailin Tao[1,2,3]

[1]The State Key Clinical Specialty in Allergy, the Second Affiliated Hospital of Guangzhou Medical University, [2]Guangdong Provincial Key Laboratory of Allergy & Clinical Immunology and [3]The State Key Laboratory of Respiratory Disease, Guangzhou Medical University, Guangzhou; [4]Department of Gastroenterology, The First Affiliated Hospital, Sun Yat-Sen University, Guangzhou, China

Purpose: Cell-in-cell structures are created by one living cell entering another homotypic or heterotypic living cell, which usually leads to the death of the internalized cell, specifically through caspase-dependent cell death (emperitosis) or lysosome-dependent cell death (entosis). Although entosis has attracted great attention, its occurrence is controversial, because one cell line used in its study (MCF-7) is deficient in caspase-3. **Methods:** We investigated this issue using MCF-7 and A431 cell lines, which often display cell-in-cell invasion, and have different levels of caspase-3 expression. Cell-in-cell death morphology, microstructures, and signaling pathways were compared in the two cell lines. **Results:** Our results confirmed that MCF-7 cells are caspase-3 deficient with a partial deletion in the *CASP-3* gene. These cells underwent cell death that lacked typical apoptotic properties after staurosporine treatment, whereas caspase-3-sufficient A431 cells displayed typical apoptosis. The presence of caspase-3 was related neither to the lysosome-dependent nor to the caspase-dependent cell-in-cell death pathway. However, the existence of caspase-3 was associated with a switch from lysosome-dependent cell-in-cell death to the apoptotic cell-in-cell death pathway during entosis. Moreover, cellular hypoxia, mitochondrial swelling, release of cytochrome C, and autophagy were observed in internalized cells during entosis. **Conclusion:** The occurrence of caspase-independent entosis is not a cell-specific process. In addition, entosis actually represents a cellular self-repair system, functioning through autophagy, to degrade damaged mitochondria resulting from cellular hypoxia in cell-in-cell structures. However, sustained autophagy-associated signal activation, without reduction in cellular hypoxia, eventually leads to lysosome-dependent intracellular cell death.

Key Words: *Autophagy, Caspase 3, Cell hypoxia, Entosis, MCF-7 cells*

INTRODUCTION

Cell death is an important physiological process involved in development and differentiation as well as the pathogenesis of certain diseases. It can be classified into three main categories including necrosis, apoptosis, and autophagy [1]. Each process is distinct in terms of cell morphology and associated signaling mechanisms. Recent research on cell death has revealed several new unique processes including intracellular death processes occurring in cell-in-cell structures [2,3]. Cell-in-cell structures are formed by one cell entering another homotypic or heterotypic cell; this leads to diverse fates for the internalized cell, but cell-in-cell death is a common outcome [4]. To date, two main types of cell-in-cell death pathways have been reported, including caspase-dependent cell-in-cell apoptotic death (emperitosis) [5] and nonapoptotic lysosome-dependent cell-in-cell death (entosis) [2]. The mechanism and potential biological significance of cell-in-cell death have been discussed [6,7] but the key factors that determine which intracellular cell death pathway is utilized are still unclear.

When the word "entosis" was first coined, it was defined as a new type of cell death utilizing a caspase-independent, nonapoptotic, lysosomal pathway, and was observed during the homotypic cell-in-cell death of tumor cells [2]. Soon after, entosis was revealed to likely be an autophagic behavior of tumor cells (outer cells) during cell starvation and other adverse conditions, because autophagy-associated mechanisms were found to be involved in the process [8]. However, during our

Correspondence to: **Ailin Tao**
The State Key Clinical Specialty in Allergy, the Second Affiliated Hospital of Guangzhou Medical University, Guangdong Provincial Key Laboratory of Allergy & Clinical Immunology, The State Key Laboratory of Respiratory Disease, Guangzhou Medical University, 250# Changgang Road East, Guangzhou 510260, China
Tel: +86-20-34153901, Fax: +86-20-34153920
E-mail: taoailin@gzhmu.edu.cn

This work was supported by the National Natural Science Foundation of China (81373128), the National Natural Science Foundation of China (81402025) and Guangdong Provincial Public Welfare Research and Capacity Building Special Fundation (2014A020212363).

Received: December 15, 2015 **Accepted:** July 20, 2016

http://ejbc.kr | pISSN 1738-6756
eISSN 2092-9900

research of cell-in-cell death, similar intracellular cell death processes were also observed during heterotypic cell-in-cell interactions between tumor cells and immune cells such as CCRF, RAJI, and MOLT4 cell lines [9]. In our previously published research, we verified that emperitosis occurs in heterotypic cell-in-cell structures observed with tumor cells and cytotoxic immune cells, and is related to the release of granzyme B by immune cells [5]. However, in the case of entosis, which occurs in both homotypic and heterotypic cell-in-cell structures, the ultimate cause of intracellular cell death cannot easily be distinguished. Thus, some interesting questions have arisen regarding the number of cell-in-cell death pathways and the factors that ultimately cause the death of internalized cells.

The Nomenclature Committee on Cell Death reclassified the categories of cell death in 2009 according to unified morphological criteria [1]. Entosis is listed as one type of cell death; however, this classification is contentious. This is mainly due to the fact that the tumor cell line MCF-7, used to describe cell-in-cell death by Overholtzer et al. [2], is deficient in caspase-3 [10]; this potentially limits its usefulness in elucidating the mechanisms of cell-in-cell death processes. The MCF-7 line is a breast cancer-derived cell line widely used to study apoptosis. However, the expression of caspase-3 in MCF-7 cells is controversial [11-13]. Considering the observation that MCF-7 cells undergo both homotypic and heterotypic cell-in-cell structure formation under different circumstances [2,9], whether caspase-3 activity affects subsequent cell-in-cell death pathways is worth exploring.

In the present study, we utilized features of MCF-7 cells to determine the role of caspase-3 in the selection of cell-in-cell death pathways. We also investigated the initiation factors that might be involved in the selection of nonapoptotic cell-in-cell death pathways. More importantly, through comparing the features of MCF-7 cells undergoing cell death inside other cells or exhibiting independent cell death, we will clarify whether MCF-7 cell-in-cell death is due to caspase-3 deficiency or if it is determined by the unique genotype of the cells. Our conclusions will yield useful information for future research of cell death, particularly in the MCF-7 cell line.

METHODS

Cell culture

The A431 cell line was purchased from the American Type Culture Collection (Manassas, USA), and was routinely maintained in DMEM (Invitrogen, Carlsbad, USA) supplemented with 10% fetal bovine serum (Hyclone, Logan, USA), and 100 units/mL penicillin plus 100 μg/mL streptomycin (Invitrogen) at 37°C with 10% CO_2. MCF-7 cells were purchased from the Chinese Academy of Sciences cell bank (Shanghai, China), and maintained under the same conditions with the addition of 0.01 mg/mL bovine insulin.

Sequencing of human *CASP-3* gene fragments

Genomic DNA was isolated from A431 and MCF-7 cells with an Animal Genomics DNA Mini Preparation Kit (New Probe, Shanghai, China). A set of primers (Y3 and Y2) that is specific for the deleted sequence of the *CASP-3* gene (designed by Jänicke [10]) was used to amplify DNA fragments from cells. Primer sequences were: forward primer (Y3), 5′-AAAGGATCCAAAGATCATACATGGAAGCGAATCAAT-3′ (+317 to +343); reverse primer (Y2), 5′-AAAGAATTCCAGTGCTTTTATGAAAATTCTTATTAT-3′ (+440 to +415). Polymerase chain reaction (PCR) products were subjected to sequencing for the determination *CASP-3* deletion.

Quantitative real-time PCR

Total RNA was extracted using the Blood RNA kit (Omega Bio-tek Inc., Norcross, USA), and reverse transcription-PCR was performed routinely with the PrimeScript real-time-PCR Kit (Takara Bio Inc., Shiga, Japan) for the preparation of *CASP-3* cDNA. The primers used for the amplification of the entire *CASP-3* coding region (Y1 and Y5) were reported previously [7]: forward primer (Y1), 5′-AAAGGATCCTTAATAAAGGTATCCATGGAGAACACT-3′ (corresponding to -15 to +12 of human *CASP-3* mRNA); and reverse primer (Y5), 5′-AAAGAATTCTTAGTGATAAAAATAGAGTTCTTTTGTGAG-3′ (+834 to +805 of human *CASP-3* mRNA).

Western blotting

Total protein was extracted from A431 and MCF-7 cell lines and was subjected to sodium dodecyl sulfate polyacrylamide gel electrophoresis (SDS-PAGE). Proteins were then transferred to nitrocellulose membranes. Membranes were probed separately with anti-pro-caspase-3 (Millipore, Billerica, USA) and anti-activated caspase-3 (Millipore) antibodies to detect the expression of caspase-3. Anti-actin (Abcam, Cambridge, USA) and anti-tubulin (Calbiochem, Darmstadt, Germany) antibodies were used as internalized controls. Immunoreactive bands were visualized by enhanced chemiluminescence (Pierce, Rockford, USA) according to the manufacturer's instructions.

Cell transfection

A caspase-3 expression plasmid (GeneCopoeia, Guangzhou, China) was transfected into MCF-7 cells using Lipofectamine® 3000 (Invitrogen). The expression of caspase-3 could be observed by fluorescence microscopy because a green fluores-

http://dx.doi.org/10.4048/jbc.2016.19.3.231

cent protein (GFP)-tag was fused to the caspase-3 protein. Western blotting was utilized to confirm the expression of caspase-3, 24 hours after transfection.

Cell death assay

Apoptosis in A431 and MCF-7 cells was induced by treatment with 1 μM of staurosporine (Calbiochem), which is a commonly used apoptosis-inducing reagent [14], for 8 to 16 hours. Terminal-deoxynucleoitidyl transferase mediated nick end labeling (TUNEL) analysis was performed using the Dead End™ Fluorimetric TUNEL System (Promega, Madison, USA). The percentage of dead cells was calculated from 100 cells, in triplicate. Cell-in-cell apoptotic rate was calculated as followed:

Apoptotic rate % = (TUNEL positive internalized cells/total cell-in-cells) × 100%

Lactate dehydrogenase (LDH) cytotoxicity analysis was performed using the CytoTox-ONE™ Homogeneous Membrane Integrity Assay according to the manufacturer's instruction (Promega).

Cell cycle analysis

Staurosporine-treated or untreated cells were fixed in precooled 80% ethanol, washed with phosphate buffered saline (PBS), and stained with 50 μg/mL of propidium iodide (PI; Sigma, St. Louis, USA) at 37°C for 60 minutes in the presence of RNase (20 μg/mL; Sigma) and 0.1% Triton X-100. Cell cycle analysis was performed using the Beckman FACScan (Brea, USA). LysoTracker™ Red and cathepsin B rates were calculated in the same manner as the TUNEL positive rate described above.

DNA fragmentation

Total DNA was extracted using the KeyGen Blood and Cell Culture Mini DNA kit (Nanjing KeyGen Biotech, Nanjing, China). Purified DNA was incubated with 200 μg/mL of RNase at 37°C for 2 hours and analyzed on 1.6% agarose gels. DNA fragments were visualized by ethidium bromide staining.

Cathepsin B activity assay

Cells seeded on coverslips were incubated with LysoTracker™ Red (Invitrogen) or the fluorogenic substrate of cathepsin B (Invitrogen) at 37°C for 30 minutes, according to the manufacturer's instructions. Cells were then fixed with freshly prepared 4% paraformaldehyde in PBS and rinsed three times in PBS. Coverslips were supported on slides using ProLong® Gold antifade reagent with 4′,6′-diamidino-2-phenylindole (DAPI) reagent (Invitrogen) and mounted using Vectashield (Vector Laboratories, Burlingame, USA; Reactolab, Servion, Switzerland). Images were taken using a fluorescence microscope (Leica, Allendale, USA). In some experiments, concanamycin A (con A; Merck), a specific inhibitor of vacuolar-type H+-ATPase (V-ATPase), which can inhibit lysosome function in both MCF-7 and A431 cells in culture [15], was used at a concentration of 100 nM to determine lysosomal activity.

Cell-in-cell internalization assays

Cell lines were stained with CellTracker™ Green dye (Invitrogen) or CellTracker™ Red dye (Invitrogen) for 30 minutes at 37°C in the absence of serum and washed with PBS three times. The cell-in-cell structures were counted using fluorescence microscopy.

Immunofluorescence assay

For immunofluorescence after internalization, cells were seeded on sterile, acid-treated, 12-mm coverslips in 24-well plates (Corning Glass Works, Corning, USA) for at least 12 hours, and then incubated with homotypic tumor cells as indicated in the legends. The cell mixtures were fixed immediately after incubation in freshly prepared 4% paraformaldehyde in PBS and rinsed three times with PBS. After blocking with PBS-0.05% Tween 20 (PBST) containing 1% bovine serum albumin (Sigma), these cells were incubated with antibodies in a humidified chamber for 1 hour, and then washed three times with TPBS. DNA was stained with DAPI (Sigma). Coverslips were supported on slides by grease pencil markings and mounted using Vectashield. Images were taken as described before. Antibodies against cleaved caspase-3 (Millipore) and Cytochrome C (Millipore) were used.

Electron microscopic analyses

After incubation for the indicated times, the cell mixture was harvested by centrifugation and fixed in cacodylate buffer (0.2 mol/L; pH 7.2) containing 2.5% glutaraldehyde (Sigma) and 1% $H_2[OsO_4(OH)_2]$ (Sigma). After dehydration, a cell monolayer was embedded in epoxy resin (Baoman, Shanghai, China) *in situ*. Ultrathin sections (70 nm) were counterstained with 50% lead citrate for 10 minutes and uranyl acetate for 30 minutes. Samples were observed with a Hitachi electron microscope (Hitachi Ltd., Tokyo, Japan).

Statistical analysis

Statistical analysis was performed with SPSS version 22.0 software (IBM Corp., Armonk, USA). Data are presented as mean ± standard deviation. A paired t-test was used to determine the p-value. A $p < 0.05$ was considered statistically significant.

RESULTS

A431 and MCF-7 cell lines were selected for typical entosis

During our study of cell-in-cell structure formation in many different cell lines, we found that the epidermoid carcinoma cell line A431 showed a high rate of homotypic cell-in-cell structure formation that was similar to that seen in MCF-7 cells cultured *in vitro*. Further TUNEL staining showed that intracellular cell death of both A431 and MCF-7 cells led to nuclear DNA degradation, as was initially used to describe entosis (Figure 1A and B). Immunofluorescence analysis was used to detect the activation of caspase-3, whereas the fluorescent substrate cathepsin B and LysoTracker™ stain were used to detect the activation of lysosomes. Our results demonstrated that during homotypic cell-in-cell interactions, the activation of caspase-3 was not observed in either cell lines, whereas strong fluorescent signals for cathepsin B and LysoTracker™ were observed in internalized cells after only 6 hours of incubation for both A431 and MCF-7 cells (Figure 1A, C, D). In addition, the fluorescent images representing cathepsin B and LysoTracker™ staining indicated that during the early stage of cell-in-cell formation, there was a marked increase in LysoTracker™ Red fluorescence in the cytoplasm of the internalized cell and an abundance of cathepsin B, released from the lysosome, permeated throughout the internalized cells. During the cell-in-cell process, we also observed lysosomal staining in the engulfing cell surrounding the double membrane vesicles of the internalized cell (Figure 1C). Therefore, we concluded that both A431 and MCF-7 cells undergo typical lysosome-dependent cell-in-cell death, and thus can be used to investigate the determining factors leading to entosis.

Partial deletion of the *CASP-3* gene in MCF-7 cells

To clarify the deficiency of *CASP-3* in MCF-7 cells, we amplified *CASP-3* genomic DNA as well as cDNA from MCF-7 cells using different pairs of primers, using caspase-3-sufficient A431 cells used as a positive control. To our surprise, PCR fragments from both genomic DNA and cDNA of MCF-7 cells were obvious after amplification, but were shorter compared to those from A431 cells (Figure 2A and B). Sequencing results indicated that there was a 47-base pair deletion between nucleotides 345 and 391 in the *CASP-3* gene (5′-GACTCTGGAATATCCCTGGACAACAGTTATAAAATG-GATTATCCTGA-3′), located at the end of exon 4, in MCF-7 cells. This deletion corresponded to +82 to +128 nucleotides in human *CASP-3* mRNA at the beginning of the translational regions (Figure 2B). More importantly, this deletion led to an in-frame, premature translational stop codon, which suggests a complete loss of the protein product. In contrast, the same deletion in the *CASP-3* gene was absent in A431 cells (used in our previous study on heterotypic cell-in-cell structures).

Subsequently, we examined the expression of a pro-caspase-3 in these two tumor cell lines by Western blotting. Our results clearly showed the presence of 32-kDa pro-caspase-3 in A431 but not in MCF-7 cells (Figure 2C), indicating that the 46-bp deletion in the *CASP-3* gene resulted in an overall deficiency of caspase-3 in MCF-7 cells.

MCF-7 cells underwent atypical apoptosis

We further evaluated the effect of caspase-3 deficiency on the induction of apoptosis. Following treatment for 16 hours with staurosporine, the activation of caspase-3 was detectable only in A431 cells but not in MCF-7 cells (Figure 3A). However, the results from the LDH cell death assay showed that the complete loss of the 17-kDa subunit in MCF-7 cells did not prevent cell death. No significant difference in the mortality rates of MCF-7 and A431 (78.7% ± 2.6% vs. 81.3% ± 3.9%, respectively) was observed after 16 hours of treatment with staurosporine (Figure 3B).

To compare the morphological and cellular characteristics of cell death, with or without caspase-3, DAPI staining and TUNEL staining were used to analyze the nuclear morphology after staurosporine treatment. Fluorescence images showed that both MCF-7 and A431 cells displayed strong TUNEL positive signals after treatment with staurosporine. Positive labeling was observed in 58.2% ± 7.7% of A431 cells and 48.7% ± 5.5% of MCF-7 cells after 16 hours of staurosporine treatment; negligible staining was observed in untreated cells (Figure 3C and 3), which was consistent with the results from the LDH assay. However, we found that there were dramatic differences in cell nucleus morphologies in A431 compared to MCF-7 cells after treatment (Figure 3D). The nuclei of A431 cells displayed the typical apoptotic morphology with obvious nuclear pyknosis after 8 hours of treatment with staurosporine. In contrast, nuclear pyknosis was not obvious in MCF-7 cells, wherein the chromosomes were disperse and loosening as indicated by the steadily paler DAPI staining. A remarkable sub-G1 apoptotic peak was consistently present in A431 cells after PI staining (Figure 3E). In addition, DNA ladder formation was evident by agarose gel electrophoresis (Figure 3F). However, there was a complete absence of the sub-G1 apoptotic peak and DNA ladder formation in dying MCF-7 cells.

Our results suggested that MCF-7 and A431 cells display distinct cell death properties after the induction of apoptosis by staurosporine. As staurosporine is a typical apoptosis-inducing reagent, this difference might be attributed to different caspase-3 expression levels between these two cell lines.

http://dx.doi.org/10.4048/jbc.2016.19.3.231

Figure 1. Lysosome-dependent cell-in-cell death of A431 and MCF-7 cell lines. (A) Kinetic quantification of internalized terminal-deoxynucleotidyl transferase mediated nick end labeling (TUNEL) positive cells, internalized cells containing cleaved caspase-3 and internalized cells demonstrating lysosome activation in cell-in-cell structures of A431 cells and MCF-7 cells. One representative experiment of three independent experiments is shown. Data are presented as means±SD. (B) Confocal images show TUNEL positive (green) and DNA fragmentation (blue) of internalized A431 cells (red) and MCF-7 cells (red) at 48 hours. Both internalized A431 and MCF-7 showed inconspicuous changes in cell size and gradual nuclei degradation after entosis. Nuclei were labeled with 4',6-diamidino-2-phenylindole (DAPI). The scale bars are 10 μm. (C) As early as 6 hours after cell engulfment, the release of active cathepsin B (red) from the lysosomes into the plasma of the internalized cells was detected and was also seen in the surrounding cytoplasm of outer cells. Cells were stained with CellTracker™ Green and cell nuclei were labeled with DAPI. The scale bars are 10 μm. (D) A431 cells (green) and MCF-7 (green) cells are stained for lysosomes using LysoTracker™ Red (red), which binds to acidified compartments after 30 hours of culture. Confocal images show positive staining for cathepsin B in the cytoplasm of internalized cells. Scale bars are 10 μm.

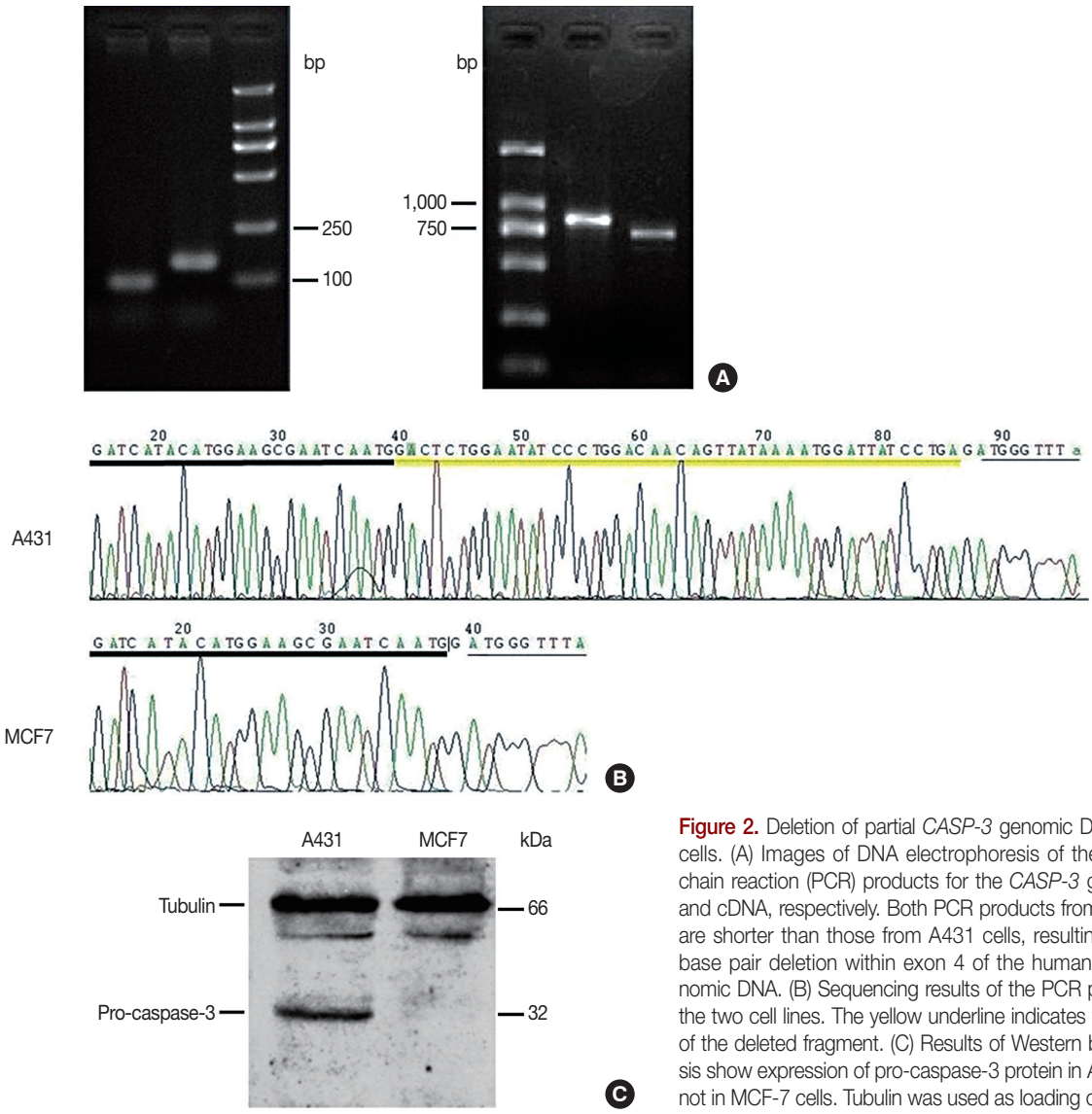

Figure 2. Deletion of partial *CASP-3* genomic DNA in MCF-7 cells. (A) Images of DNA electrophoresis of the polymerase chain reaction (PCR) products for the *CASP-3* genomic DNA and cDNA, respectively. Both PCR products from MCF-7 cells are shorter than those from A431 cells, resulting from a 47-base pair deletion within exon 4 of the human *CASP-3* genomic DNA. (B) Sequencing results of the PCR products from the two cell lines. The yellow underline indicates the sequence of the deleted fragment. (C) Results of Western blotting analysis show expression of pro-caspase-3 protein in A431 cells but not in MCF-7 cells. Tubulin was used as loading control.

Entosis converting to apoptosis in the presence of caspase-3

To further determine the role of caspase-3 in the transition from lysosome-dependent cell death to caspase-dependent cell death, entosis was interrupted by treatment with 100 nM con A. Samples were simultaneously prepared for the detection of cleaved caspase-3. Our results showed that when lysosome activity was inhibited, caspase-3 sufficient A431 cells predominantly switched from lysosome-dependent cell-in-cell death to caspase-3-dependent cell-in-cell apoptosis (Figure 4A). DAPI staining showed that the nuclear morphology of A431 cells after intracellular cell death switched from DNA fragmentation to typical apoptotic chromatin condensation. However, the absence of caspase-3 in MCF-7 cells impeded this cell in-cell death transition, and these cells maintained their nuclear morphology and DNA fragmentation typically observed in entosis. We next transfected pEZ-*CASP3* to MCF-7 cells to express caspase-3 in MCF-7 cells (Figure 4B). Cleaved caspase-3 activity was then assessed in MCF-7 cells and caspase-3 expressing MCF-7 cells during apoptosis induced by staurosporine and during cell-in-cell death after inhibiting lysosome activity with con A (Figure 4A and C). To compare the cell death transition, with or without lysosome activity, intracellular cell death was observed by TUNEL staining in MCF-7 cells, caspase-3 expressing MCF-7 cells, and in A431 cells with or without the inhibition of con A (Figure 4D). Results showed no significant difference in terms of the cell death transition between caspase-3 expressing MCF-7 and A431 cells. Intracellular death in MCF-7 cells decreased after 48 hours of con A treatment but this was statistically insignificant (Figure 4D). In summary, the above results revealed that

http://dx.doi.org/10.4048/jbc.2016.19.3.231

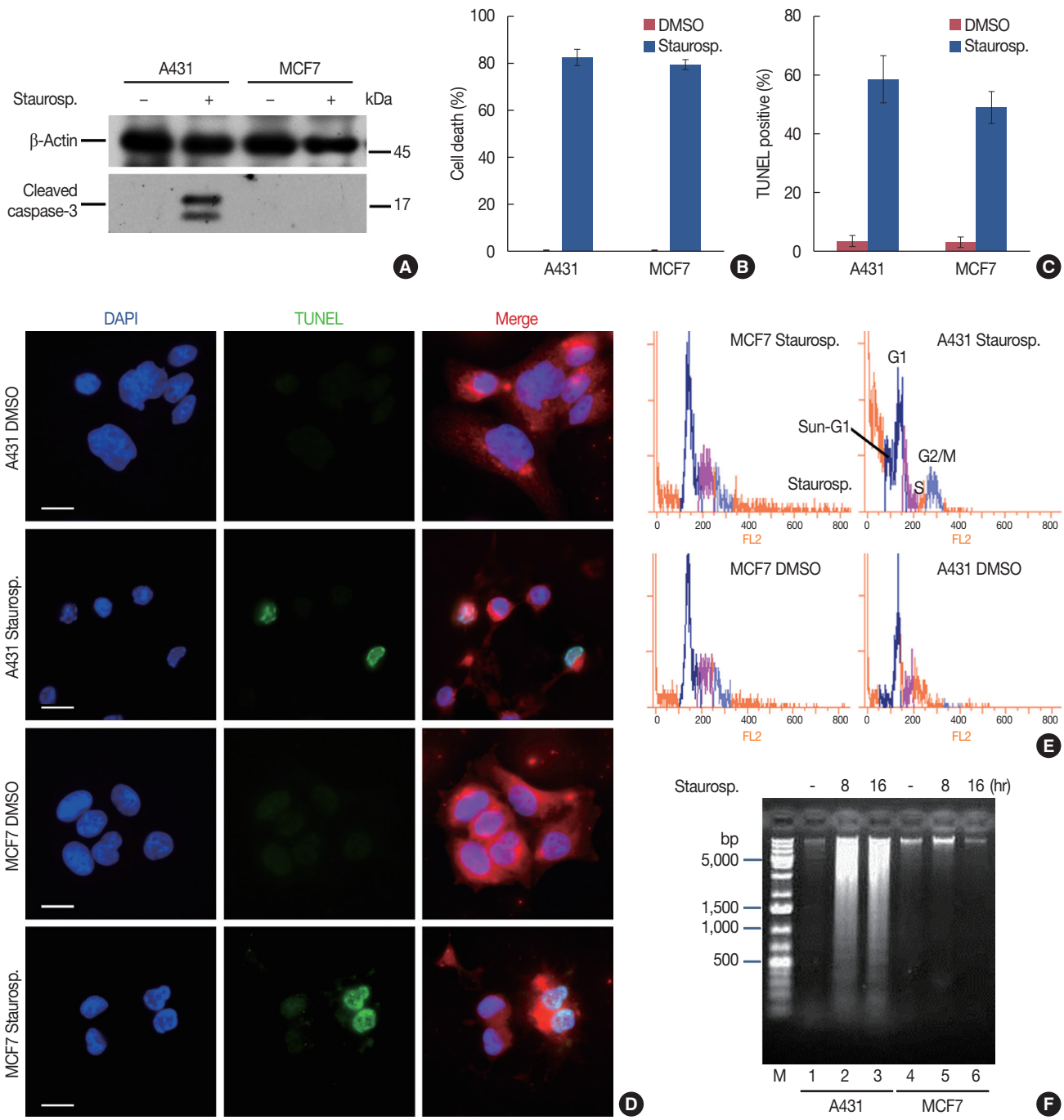

Figure 3. Absence of caspase-3 protein in MCF-7 cells leading to an atypical apoptosis. (A) Expression of cleaved caspase-3 protein in A431 cells but not in MCF-7 cells. Both tumor cell lines were treated with (+) or without (–) staurosporine (staurosp.) for 16 hours and the cell lysates were analyzed by Western blotting. β-Actin was used as loading control. (B) Cytotoxicity assays of A431 and MCF-7 cells using the LDH method after treatment with staurosporine for 16 hours. Cells treated with the solvent dimethyl sulphoxide (DMSO) were used as negative controls. (C) Terminal-deoxynucleoitidyl transferase mediated nick end labeling (TUNEL) assay showed similar mortalities of the two cell lines following treatment with staurosporine for 16 hours. (D) Confocal images show positive TUNEL staining in both A431 and MCF-7 cells after treatment with staurosporine. Nuclear pyknosis was obvious in dying A431 cells but not in dying MCF-7 cells. Cells were labeled with CellTracker™ Red, and cell nuclei were stained with 4',6-diamidino-2-phenylindole (DAPI). The scale bars are 10 μm. (E) Cell cycle analysis of A431 and MCF-7 cells treated with or without staurosporine for 8 hours. The sub-G1 apoptotic peak demonstrating nuclear pyknosis in apoptotic cells is seen before the G0/G1 peak in A431 cells but not in MCF-7 cells after apoptosis induction. (F) DNA was prepared from cells untreated or treated for 8 hours or 16 hours with staurosporine and analyzed using a 1.6% agarose gel. There was obvious DNA ladder formation in A431 but not in MCF-7 cells after apoptosis induction. Lane M: DNA ladder.

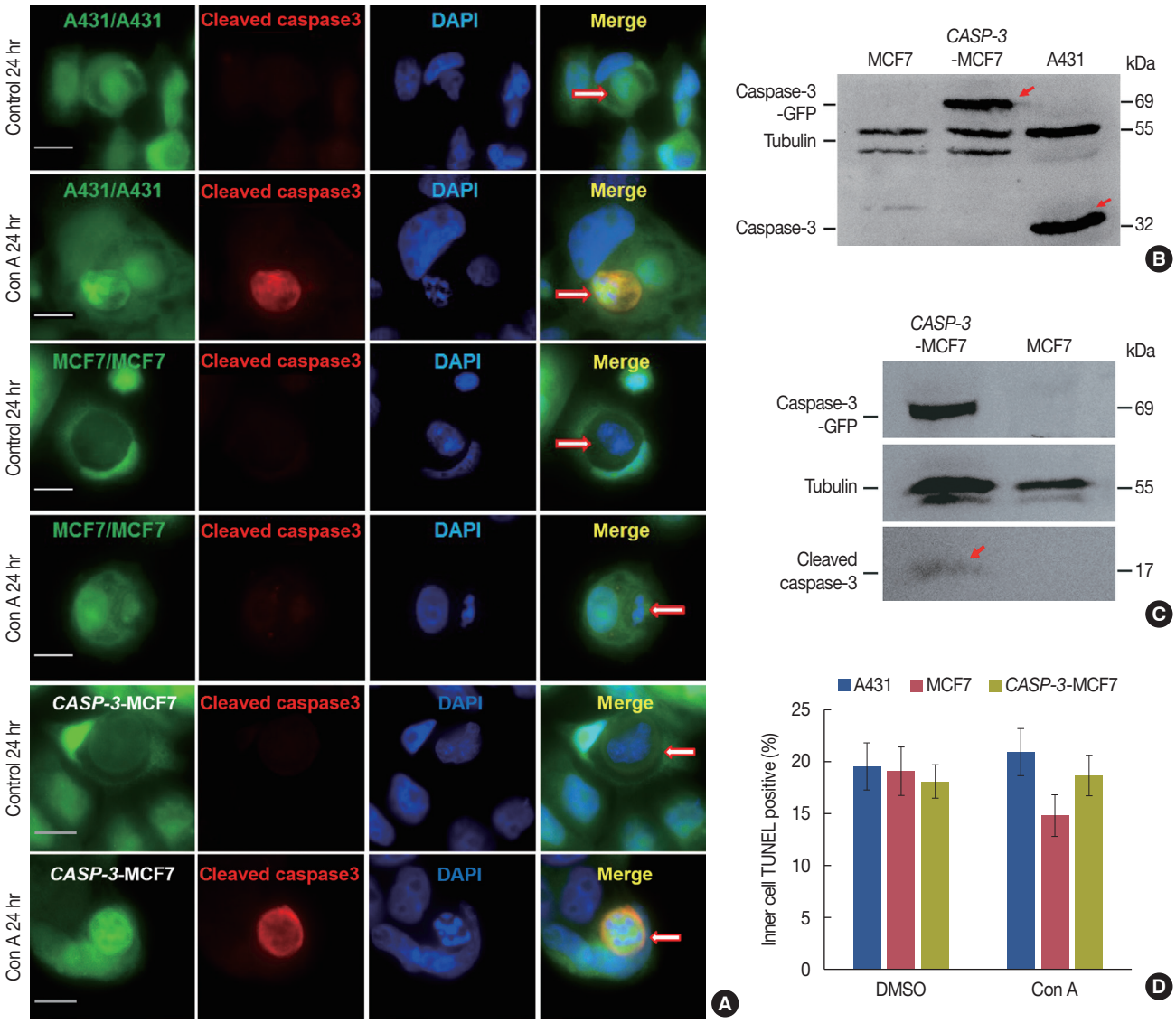

Figure 4. Entosis converting to apoptosis in the presence of caspase-3. (A) Immunofluorescence of cleaved caspase-3 activity in A431 cells, caspase-3 expressing MCF-7 cells and MCF-7 cells with or without concanamycin A (con A) treatment. The three kinds of cells showed typical lysosomal cell-in-cell death before treatment. After treatment we could see clear caspase-3 activation, nuclear shrinkage, nuclear pyknosis and other apoptotic forms in A431 and caspase-3 expressing MCF-7 cells. In contrast, no caspase-3 activity or other apoptosis characteristics was detected in MCF-7 cells after the same treatment. These pictures were taken after 24 hours of cell incubation. The scale bars are 10 μm. Arrows point to entosis cells. (B) Result of Western blot showed fusion protein caspase-3-green fluorescent protein (GFP) (arrows marked) expressed in caspase-3 expressing MCF-7 cells which was about 69 kDa. (C) Result of Western blotting showed caspase-3-GFP (69 kDa) and cleaved caspase-3 (17 kDa, arrow marked) were detected in caspase-3 expressing MCF-7 cells but not in MCF-7 cells. Both of the cells were treated with staurosporine for 16 hours. (D) Statistical analysis of cell-in-cell death of A431 cells, caspase-3 expressing MCF-7 cells and MCF-7 cells with or without Concanamycin A treatment for 48 hours determined by terminal-deoxynucleotidyl transferase mediated nick end labeling (TUNEL) assay. Data are presented as means ± SD.

the absence of caspase-3 did indeed play a role in the death of internalized cells in cell-in-cell structures; however, it was not the determining factor because caspase-3 deficient MCF-7 cells were also able to undergo intracellular cell death in such structures even when lysosome activity was inhibited.

Cell autophagy during hypoxia leads to entosis

After observing the microstructures after cell-in-cell invasion in A431 and MCF-7 cells, we noticed that there was obvious damage to the organelles, such as mitochondrial swelling, at the early stages of internalized cell death, and a large number of autophagic vacuoles and autophagy-associated lyso-

http://dx.doi.org/10.4048/jbc.2016.19.3.231

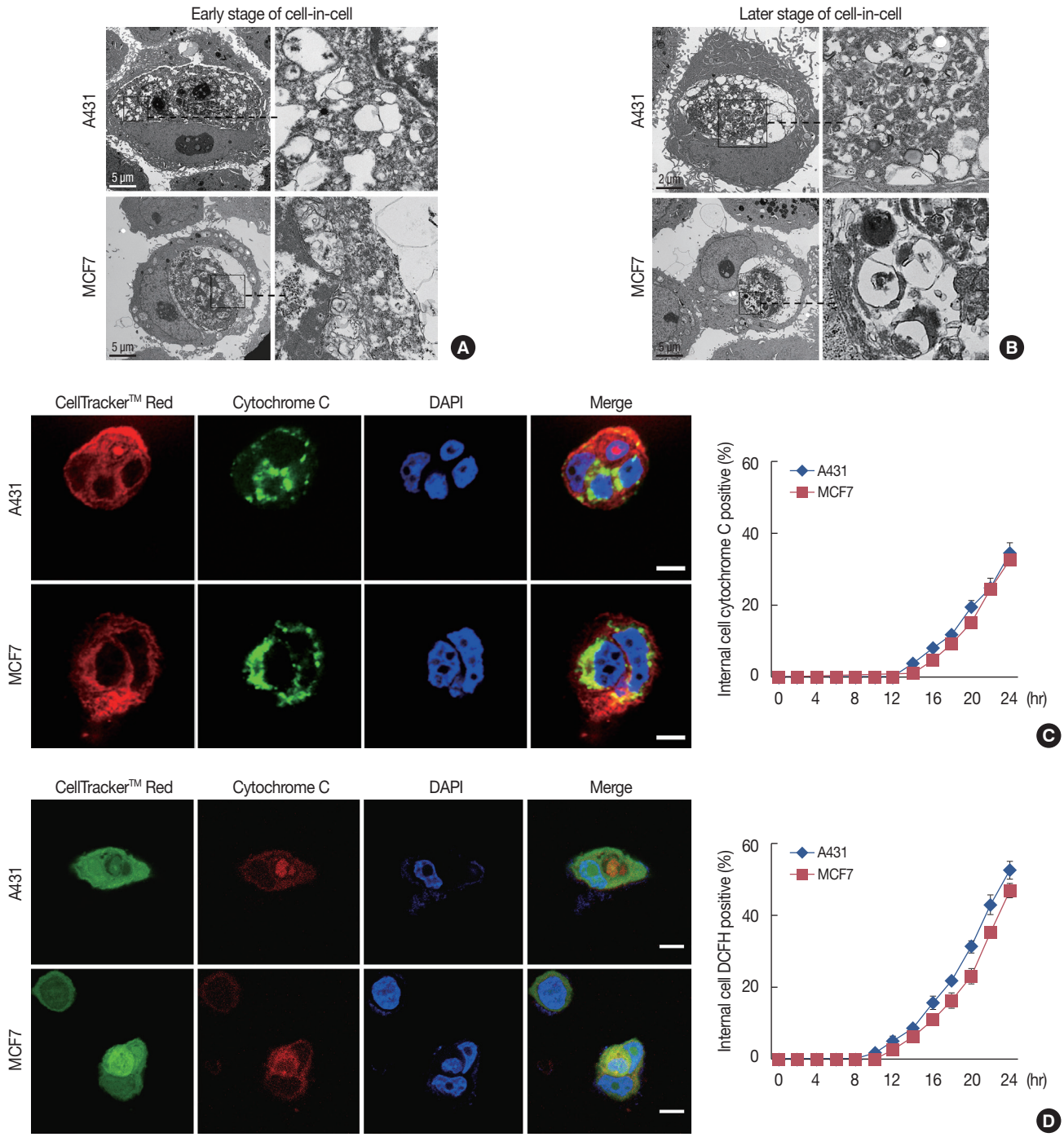

Figure 5. Cell autophagy against hypoxia leading to entosis. (A) Transmission electron microscope images show the ultrastructures of A431 and MCF-7 cells undergoing entosis. Right panels show greater details of left panels. Images show mitochondria swelling and DNA degradation of internalized cells at the early stage of cell-in-cell formation. (B) Images show internal cells completely losing their morphology with a large number of autophagic vacuoles and autophagic lysosomes at a later stage of cell-in-cell formation. (C) We used anticytochrome C antibody, which can only bind to cytochrome C released from mitochondria and indicates mitochondrial injury. Confocal images show strong fluorescence (green) in the cytoplasm of the internalized cells. Cells were labeled with CellTracker™ Red and cell nuclei were stained with DAPI. The scale bars are 10 μm. The right diagram shows the kinetics of cytochrome C release in the internalized tumor cells. (D) 2',7'-Dichlorofluorescin diacetate (DCFI-DA) was used to detect reactive oxygen species (ROS) in internalized cells of cell-in-cell structure. Confocal images show clear ROS (red) in the cytoplasm of internalized cells. Cells were labeled with CellTracker™ Green, and cell nuclei were stained with 4',6-diamidino-2-phenylindole (DAPI). The scale bars are 10 μm, which has been described in the legend in Figure 5. The right diagram displayed the kinetics of ROS positive internalized cells in cell-in-cell structures.

somes were seen during the later stages of internalized cell death (Figure 5A and B). We confirmed by immunofluorescence that cell-in-cell structure formation could lead to the release of cytochrome C from the mitochondria in internalized cells during the early stage of this process (Figure 5C). Further immunofluorescence experiments examining cell-in-cell structure formation using fluorescent sensor 2', 7'-Dichlorofluorescin diacetate (DCFH-DA), which can detect ROS in hypoxic cells, indicated the presence of hypoxia in the internalized cells, which could result in mitochondrial damage (Figure 5D).

DISCUSSION

The concept of "cell-in-cell death" is derived from the observation that living cells enter other homotypic or heterotypic cells, and subsequently die during the formation of cell-in-cell structures [4]. However, the exact molecular mechanism of cell-in-cell death is not fully known. In the present study, we demonstrated that caspase-3 deficiency, as seen in the MCF-7 cell line, results in cell-in-cell death with atypical apoptotic properties, unlike that observed in the caspase-3 sufficient A431 cell line. Moreover, the absence of caspase-3 in MCF-7 cells had little effect on lysosome-dependent cell-in-cell death during entosis or when lysosome activity was inhibited. Nevertheless, caspase-3 does indeed play a certain role in cell-in-cell death in that it causes a transition from lysosome-dependent cell-in-cell death to caspase-dependent cell-in-cell apoptosis in the caspase-3 sufficient A431 cell line. Additionally, we discovered that entosis is utilized as a type of self-repair to eliminate damaged mitochondria caused by hypoxia in cell-in-cell structures. However, sustained autophagy-associated signal activation, without alleviation of the harsh cellular microenvironment, eventually led to lysosome-dependent cell-in-cell death.

Based on the molecules involved, it has been reported that there are two types of cell-in-cell death pathways, specifically, lysosome-dependent degradation (entosis) and caspase-involved apoptosis (emperitosis). These two pathways are associated with different types of cell-in-cell structures, suggesting differential physiological significance. Benseler et al. [7] reported the cell-in-cell death of naïve autoreactive T cells in the lysosomes of hepatocytes and proposed a physiologic role for emperipolesis as a unique mechanism for deletion of autoreactive CD8 T cells that are activated in the liver. One previously reported cell death pathway, termed cannibalism, also exhibits properties similar to cell-in-cell death [16]. However, the cannibalism pathway is not the same as that observed for either homotypic or heterotypic cell-in-cell death. Cannibalism is defined as the entrance of both apoptotic and living cells into another living cell, and only partially shares characteristics with phagocytosis and entosis. Upon entering the cell, the lysosome degradation system is activated to induce cell death [6].

Lysosome-dependent degradation is mainly associated with homotypic cell-in-cell structures, especially in tumor cells. In fact, we have performed a survey using a panel of more than 100 tumor cell lines as host cells and several lymphocytes as target cells to study the mechanisms associated with cell-in-cell structures. Our published data indicates that lysosome-dependent cell-in-cell death occurs via homotypic entosis regardless of the origin or species of the cell line [9]. Hence, we inferred that cell-in-cell death might be important for tumor development. Interestingly, during heterotypic cell-in-cell interactions between immunocytes and tumor cells, lymphocytes without cytotoxic properties, such as primary CD4 T cells and B cells, underwent lysosome-dependent cell-in-cell degradation. Cell-in-cell death in cells that have killing activities, such as NK and LAK cells, is characterized by apoptotic cell-in-cell death, and might be a suicide event executed by granzyme B release from internalized killer cells [5]. All of these observations strongly suggest that the occurrence of cell-in-cell death is related to the property of the internalized cell rather than to the characteristics of the host cell. This implies that the type of cell being internalized might be the "arbiter" in determining which cell-in-cell death pathway is utilized.

It has been reported that con A, a lysosome inhibitor, could convert the entosis process, utilized by MCF-10A cells, to a caspase-dependent apoptotic process [2]. In our study, similar results were obtained in the homotypic cell-in-cell structure formed by caspase-3 sufficient A431 cells and in caspase-3-expressing MCF-7 cells, but not in caspase-3-deficient MCF-7 cells after treatment with con A, indicating that the presence of caspase-3 in cells is critical for the transition of one cell-in-cell death pathway to another. However, the absence of caspase-3 did not prevent death in MCF-7 cells in cell-in-cell structures after con A treatment. A number of MCF-7 cells underwent cell death, utilizing an atypical apoptosis pathway, but at an insignificant, slower rate, compared to that in caspase-3 expressing MCF-7 cells and in A431 cells (that underwent typical intracellular apoptosis). We conclude that there are signaling pathways, other than those associated with caspase and lysosome systems, which are able to mediate intracellular cell death.

Recently, the mechanism of lysosome-dependent entosis was revealed to be associated with autophagy [8]. However, it is still unclear what factors are regulated by autophagy signals. Considering that autophagy is a mechanism of self-repair used to clear damaged cell organelles, and that cell-in-cell

http://dx.doi.org/10.4048/jbc.2016.19.3.231

structures could create harsh environments for internalized cells, we first analyzed the microstructure of tumor cell-in-cell structures. It was apparent that there were damaged organelles in the cytoplasm of internalized tumor cells, such as swollen mitochondria, autophagic vacuoles, and autophagic lysosomes. Further studies revealed that there was significant intracellular hypoxia associated with internalized tumor cells in cell-in-cell structures. It is known that autophagy is a self-repair mechanism that is accomplished by degrading, digesting, and eliminating damaged organelles when cells are exposed to a harsh environment [17-19]. However, sustained autophagy signal activation without relief could eventually lead to programmed cell death [20-22]. Thus, we speculate that after a cell-in-cell structure forms in tumor cells, hypoxia eventually occurs in the internalized cell, and leads to organelle damage. Consequently, the autophagy program is initiated through activation of the lysosome and autophagosome to clear damaged organelles, for survival during the hypoxia crisis. However, it also results in irreversible injury to the internalized cell and eventually leads to its death via a lysosome-dependent pathway. In summary, we conclude that entosis is an overreaction of internalized cells attempting to save themselves by utilizing autophagy mechanisms when exposed to hypoxic conditions in cell-in-cell structures.

In conclusion, the results described here clarify the fact that lysosome-dependent and apoptotic cell-in-cell death pathways are two independent pathways triggered by different factors that are derived from internalized cells. Dissecting the precise mechanisms of these two cell-in-cell death pathways as well as their physiological and pathological significance will enrich the present knowledge and understanding of cell death in different situations.

CONFLICT OF INTEREST

The authors declare that they have no conflict of interests.

REFERENCES

1. Kroemer G, Galluzzi L, Vandenabeele P, Abrams J, Alnemri ES, Baehrecke EH, et al. Classification of cell death: recommendations of the Nomenclature Committee on Cell Death 2009. Cell Death Differ 2009;16:3-11.
2. Overholtzer M, Mailleux AA, Mouneimne G, Normand G, Schnitt SJ, King RW, et al. A nonapoptotic cell death process, entosis, that occurs by cell-in-cell invasion. Cell 2007;131:966-79.
3. Wang S, Guo Z, Xia P, Liu T, Wang J, Li S, et al. Internalization of NK cells into tumor cells requires ezrin and leads to programmed cell-in-cell death. Cell Res 2009;19:1350-62.
4. Overholtzer M, Brugge JS. The cell biology of cell-in-cell structures. Nat Rev Mol Cell Biol 2008;9:796-809.
5. Wang S, He MF, Chen YH, Wang MY, Yu XM, Bai J, et al. Rapid reuptake of granzyme B leads to emperitosis: an apoptotic cell-in-cell death of immune killer cells inside tumor cells. Cell Death Dis 2013;4:e856.
6. Fais S. Cannibalism: a way to feed on metastatic tumors. Cancer Lett 2007;258:155-64.
7. Benseler V, Warren A, Vo M, Holz LE, Tay SS, Le Couteur DG, et al. Hepatocyte entry leads to degradation of autoreactive CD8 T cells. Proc Natl Acad Sci U S A 2011;108:16735-40.
8. Florey O, Kim SE, Sandoval CP, Haynes CM, Overholtzer M. Autophagy machinery mediates macroendocytic processing and entotic cell death by targeting single membranes. Nat Cell Biol 2011;13:1335-43.
9. Chen YH, Wang S, He MF, Wang Y, Zhao H, Zhu HY, et al. Prevalence of heterotypic tumor/immune cell-in-cell structure in vitro and in vivo leading to formation of aneuploidy. PLoS One 2013;8:e59418.
10. Jänicke RU. MCF-7 breast carcinoma cells do not express caspase-3. Breast Cancer Res Treat 2009;117:219-21.
11. Feng FF, Zhang DR, Tian KL, Lou HY, Qi XL, Wang YC, et al. Growth inhibition and induction of apoptosis in MCF-7 breast cancer cells by oridonin nanosuspension. Drug Deliv 2011;18:265-71.
12. Chen JS, Konopleva M, Andreeff M, Multani AS, Pathak S, Mehta K. Drug-resistant breast carcinoma (MCF-7) cells are paradoxically sensitive to apoptosis. J Cell Physiol 2004;200:223-34.
13. Jänicke RU, Sprengart ML, Wati MR, Porter AG. Caspase-3 is required for DNA fragmentation and morphological changes associated with apoptosis. J Biol Chem 1998;273:9357-60.
14. Langford MP, Chen D, Gosslee J, Misra RP, Redens TB, Texada DE. Intracameral toxicity of bacterial components muramyl dipeptide and staurosporine: ciliary cyst formation, epithelial cell apoptosis and necrosis. Cutan Ocul Toxicol 2006;25:85-101.
15. Li M, Khambu B, Zhang H, Kang JH, Chen X, Chen D, et al. Suppression of lysosome function induces autophagy via a feedback down-regulation of MTOR complex 1 (MTORC1) activity. J Biol Chem 2013;288:35769-80.
16. Lugini L, Matarrese P, Tinari A, Lozupone F, Federici C, Iessi E, et al. Cannibalism of live lymphocytes by human metastatic but not primary melanoma cells. Cancer Res 2006;66:3629-38.
17. Rausch V, Liu L, Apel A, Rettig T, Gladkich J, Labsch S, et al. Autophagy mediates survival of pancreatic tumour-initiating cells in a hypoxic microenvironment. J Pathol 2012;227:325-35.
18. Wojtkowiak JW, Gillies RJ. Autophagy on acid. Autophagy 2012;8:1688-9.
19. Garg AD, Dudek AM, Ferreira GB, Verfaillie T, Vandenabeele P, Krysko DV, et al. ROS-induced autophagy in cancer cells assists in evasion from determinants of immunogenic cell death. Autophagy 2013;9:1292-307.
20. Macintosh RL, Ryan KM. Autophagy in tumour cell death. Semin Cancer Biol 2013;23:344-51.
21. Denton D, Nicolson S, Kumar S. Cell death by autophagy: facts and apparent artefacts. Cell Death Differ 2012;19:87-95.
22. Minina EA, Bozhkov PV, Hofius D. Autophagy as initiator or executioner of cell death. Trends Plant Sci 2014;19:692-7.